ACS OMEGA

Article

Cite This: ACS Omega 2018, 3, 667−676

Effect of Carbon Nanotubes on Direct Electron Transfer and Electrocatalytic Activity of Immobilized Glucose Oxidase

Yuxiang Liu,[†,‡] Jin Zhang,[‡] Yi Cheng,[‡] and San Ping Jiang*[,‡]

[†]College of Environmental Science and Engineering, Taiyuan University of Technology, Taiyuan 030024, China

[‡]Fuels and Energy Technology Institute & Department of Chemical Engineering, Curtin University, Perth, Western Australia 6102, Australia

ABSTRACT: Carbon nanotubes (CNTs) are excellent supports for electrocatalysts because of their large surface area, excellent electronic conductivity, and high chemical and structural stability. In the present study, the activity of CNTs on direct electron transfer (DET) and on immobilized glucose oxidase (GO_X) is studied as a function of number of walls of CNTs. The results indicate that the GO_X immobilized by the CNTs maintains its electrocatalytic activity toward glucose; however, the DET and electrocatalytic activity of GO_X depend strongly on the number of inner tubes of CNTs. The GO_X immobilized on triple-walled CNTs (TWNTs) has the highest electron-transfer rate constant, 1.22 s^{-1}, for DET, the highest sensitivity toward glucose detection, 66.11 ± 5.06 $\mu A\ mM^{-1}\ cm^{-2}$, and the lowest apparent Michaelis−Menten constant, 6.53 ± 0.58 mM, as compared to GO_X immobilized on single-walled and multiwalled CNTs. The promotion effect of CNTs on the GO_X electrocatalytic activity and DET is most likely due to the electron-tunneling effect between the outer wall and inner tubes of TWNTs. The results of this study have general implications for the fundamental understanding of the role of CNT supports in DET processes and can be used for the better design of more effective electrocatalysts for biological processes including biofuel cells and biosensors.

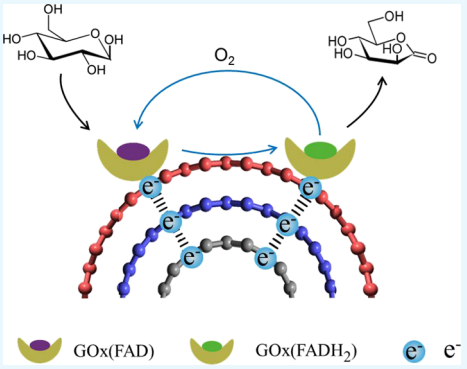

1. INTRODUCTION

Direct electrochemistry of redox enzymes/proteins such as glucose oxidase (GO_X) plays an important role in the glucose oxidation reactions in enzyme-immobilized electrodes in microbial and enzymatic fuel cells[1−5] and in glucose biosensors.[5−7] In enzymatic/microbial fuel cells and electrochemical biosensors, enzymes or microbes are generally immobilized on electrode material surfaces; however, a key issue in such systems is the efficient electron transfer (ET) between the active centers and the supporting substrate or electrode.[3,8,9] In the case of GO_X, direct ET (DET) with the bare electrode is difficult because of the fact that the redox active flavin adenine dinucleotide (FAD) cofactors, that is, small nonproteinaceous electroactive species, of GO_X are deeply buried within electrically well-insulated prosthetic shells.[10,11] Thus, considerable efforts have been made to enhance the DET of GO_X via the redox mediators and the selected matrix and to develop new and high-performance biofuel cells and enzymatic electrochemical biosensors.[3,8,12,13]

Mediators such as 2-hydroxy-1,4-naphthoquinone, thionin, ferrocene monocarboxylic acid, and methylene blue offer advantages for immobilization of enzymes and enhancement of DET capacity and power output of biofuel cells.[14−17] In mediated ET using electroactive molecules or mediators to shuttle electrons between the enzyme and the electrode, the maximum cell voltage of biofuel cells is determined by the thermodynamic redox potential of mediators. A more positive redox potential is required to provide the driving force for the ET between the enzyme active center and the electrode for the oxidation biocatalysts, which contributes to cell voltage loss. Another area of intensive research is to use advanced smart carbon materials such as carbon nanotubes (CNTs),[18−21] carbon black,[22,23] carbon nanoparticles (NPs),[24] vertically aligned CNTs,[25] and graphene,[13,26] in immobilization and growth of enzymes/proteins and living cells for various biological processes and for electrochemical biosensors and biofuel cells. Among them, CNTs have attracted considerable attention for potential applications such as supporting materials for enzymes owing to their unique electrical conductivity, high chemical stability, biocompatibility, and large surface area.[18−20,27] However, it has been shown that the physical and chemical properties of CNTs can influence the adsorption and activity of immobilized enzymes.[28,29] Pang et al. studied the effect of various carbon materials on the enzyme loading and laccase activity, including fullerene (C-60), multiwalled CNTs (MWNTs), oxidized MWNTs, and graphene oxide and found that the immobilized enzymes have significantly reduced reaction rates as compared to free laccase.[30] This has been attributed to the nanomatrix-induced diffusional limitation on the enzyme activity.

Received: October 25, 2017
Accepted: January 5, 2018
Published: January 19, 2018

DOI: 10.1021/acsomega.7b01633
ACS Omega 2018, 3, 667−676

Recently, we have found that pristine CNTs composed of 2−3 concentric tubes or walls have significantly higher electrochemical activities for O_2 evolution reactions (OERs) as compared with typical single-walled CNTs (SWNTs) and MWNTs .[31] The electrocatalytic activity of CNTs shows a distinct volcano-type curve as a function of the number of walls of CNTs. Similar volcano curves were also observed on Pt and Pd NP-supported CNTs for methanol, ethylene glycol, ethanol, and formic acid oxidation in alkaline solutions and on dye-functionalized CNTs for photoelectrochemical (PEC) water splitting.[32−35] This indicates that the number of walls or inner tubes of CNTs plays an important role in promoting the ET of the electrochemical redox reaction on the surface of CNTs, and such a promotion effect could be beneficial to the DET of the redox reactions of enzymes/proteins. Here, the effects of quantum properties of CNTs on the DET and electrocatalytic activity of GO_X toward glucose oxidation were studied. The results indicate that triple-walled CNTs (TWNTs) facilitate fast DET of GO_X and enhance the electrocatalytic activity for glucose sensing, as compared to that on SWNTs and MWNTs.

2. RESULTS AND DISCUSSION

2.1. CNTs and Direct Electrochemistry of GO_X/CNT-Modified Glassy Carbon Electrodes. Figure 1 shows the transmission electron microscopy (TEM) micrographs of the CNTs used in this study. CNTs were divided into four groups, depending on the number of walls. CNT-1 mainly consists of SWNTs (79%) with an outer diameter (OD) of 1.97 nm. CNT-2 is dominated by TWNTs (52%) and double-walled CNTs (DWNTs, 25%) with an OD of 3.80 nm. The average number of walls of CNT-3 is seven with an OD of 7.45 nm, whereas CNT-4 is a typical MWNT with an average of 12 walls and an OD of 13.9 nm. CNTs with a small OD prefer to form bundles because of the van der Waals interactions;[36] however, CNTs with a large OD, CNT-3 and CNT-4, are well-dispersed without bundles. After purification, the amount of Fe, Co, Mo, and Ni elements are substantially reduced to less than 100 ppm as confirmed by the inductively coupled plasmaoptical emission spectroscopy analysis. The details of CNTs used in this study can be found elsewhere.[32] The Brunauer−Emmett−Teller (BET) surface area of CNTs is in the range of 271−577 $m^2\ g^{-1}$. Table 1 summarizes the average number of walls and surface areas of CNTs.

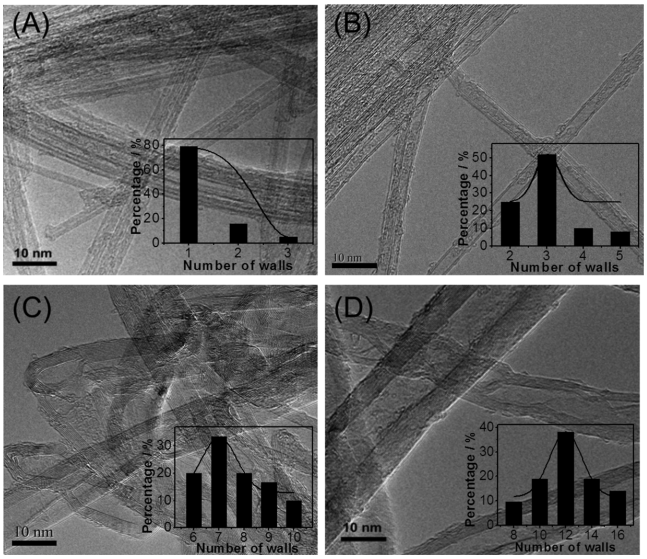

Figure 1. TEM micrographs of (A) CNT-1, (B) CNT-2, (C) CNT-3, and (D) CNT-4.

Table 1. Average OD, Average Wall Numbers (n), and the BET Surface Area (S_{BET}) of CNTs

sample	OD/nm	n	$S_{BET}/m^2\ g^{-1}$
CNT-1	1.97	1	577
CNT-2	3.80	3	523
CNT-3	6.90	7	539
CNT-4	13.8	12	271

Figure 2A shows the cyclic voltammograms (CVs) of the bare glassy carbon (GC) and CNT-modified GC electrodes in an N_2-saturated 0.1 M phosphate-buffered saline (PBS) solution at a scan rate of 50 mV s^{-1}. No reduction or oxidation peaks were observed in the CVs of both bare GC and CNT-modified electrodes. However, the CNT-modified GC electrodes show substantially high background current as compared to bare GC electrodes, indicating the high active sites of CNTs and the formation of well-integrated CNT-modified GC electrodes. In the case of GO_X/CNT-modified electrodes, a pair of well-defined and symmetrical redox peaks with equal oxidation and reduction peak heights at about −0.48 V appears (Figure 2B). It is well-known that the cofactor of GO_X, existing in two different states, FAD (oxidized form) and $FADH_2$ (reduced form), can work as an electron acceptor and donor alternatively in redox reactions.[37] The observed redox peaks indicate that FAD from GO_X can undergo reversible direct electrochemical oxidation and reduction on the GO_X/CNT-modified GC electrodes without the help of the electron-transfer mediators. On the other hand, the CV obtained from the electrode modified with GO_X only is featureless, indicating that the DET between the GC electrode and FAD, the active redox center of GO_X, is very weak without CNT modification. CNTs have the excellent electron-transport property and high special surface area, which promotes significantly the ET and facilitates the DET process between the redox center of GO_X and the GC electrode substrate as shown in this study and also by others.[18−20,37] The distinct differences of the electrochemical behavior of CNTs, GO_X, and GO_X/CNTs as shown in Figure 2 also clearly indicate the immobilization of GO_X on CNTs. The immobilization of GO_X on CNTs is most likely due to the $\pi{=}{=}\pi$ and $\sigma-\pi$ stacking, similar to that observed in the case of polyelectrolyte-functionalized CNTs.[38−41]

The oxidation and reduction peak potentials are located in the potential range between −0.431 and −0.473 V (vs Ag/AgCl). The formal potential ($E°$) of the electrodes, calculated by averaging the cathodic and anodic peak potential, is in the range of 0.449−0.458 V, which is close to the standard potential of FAD/$FADH_2$ (i.e., −0.460 V in pH 7.0 at 25.8 °C). Similar values were also reported for other GO_X-modified GC electrodes.[42,43] The separation potential of the cathodic and anodic peaks, ΔE_p, depends on the CNTs. The ΔE_p values of GO_X/CNT-1, GO_X/CNT-2, GO_X/CNT-3, and GO_X/CNT-4 are 35, 24, 31, and 34 mV, respectively. For the redox reaction on GO_X/CNTs, the ΔE_p value shows the lowest value at the GO_X/CNT-2-modified GC electrode, 0.024 V, proving a fast electron-transfer process on GO_X-immobilized CNT-2. Periasamy et al. studied the direct electrochemistry of GO_X at gelatin- and *N*,*N*-dimethylformamide (DMF)-dispersed MWNTs and GMWNT- and DMWNT-modified GC electrodes, and observed that the difference of ΔE_p

DOI: 10.1021/acsomega.7b01633
ACS Omega 2018, 3, 667−676

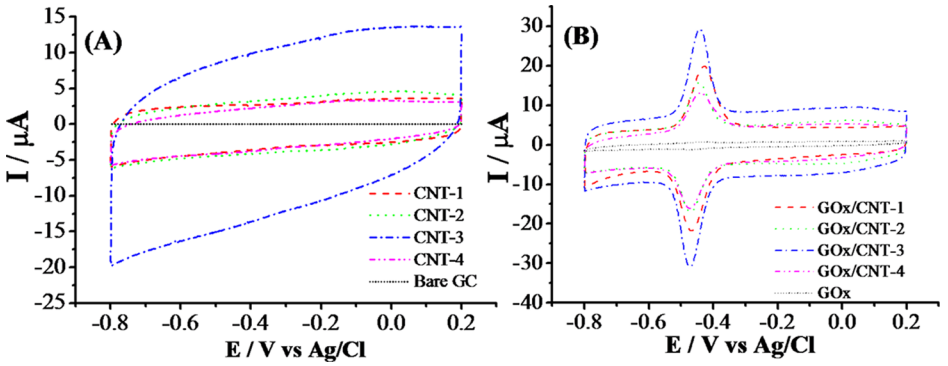

Figure 2. CVs recorded at (A) bare GC electrode and CNT-modified electrodes and (B) GO_X and GO_X/CNT-modified GC electrodes in an N_2-saturated 0.1 M PBS solution at a scan rate of 50 mV s^{-1}.

Table 2. Electrochemical Parameters for the Direct Electrochemistry of GO_X on Different GO_X/CNT-Modified GC Electrodes

	peak current (μA cm^{-2})			peak potential (V)			
electrode	anode (I_{pa})	cathode (I_{pc})	$E°$ (V)	anode (E_{pa})	cathode (E_{pc})	peak separation (ΔE_p, V)	k_s (s^{-1})
GO_X/CNT-1	158.1	−173.3	−0.449	−0.431	−0.466	0.035	0.984
GO_X/CNT-2	125.3	−136.9	−0.458	−0.446	−0.470	0.024	1.22
GO_X/CNT-3	233.7	−246.4	−0.458	−0.442	−0.473	0.031	1.064
GO_X/CNT-4	104.7	−128.6	−0.456	−0.439	−0.473	0.034	1.004

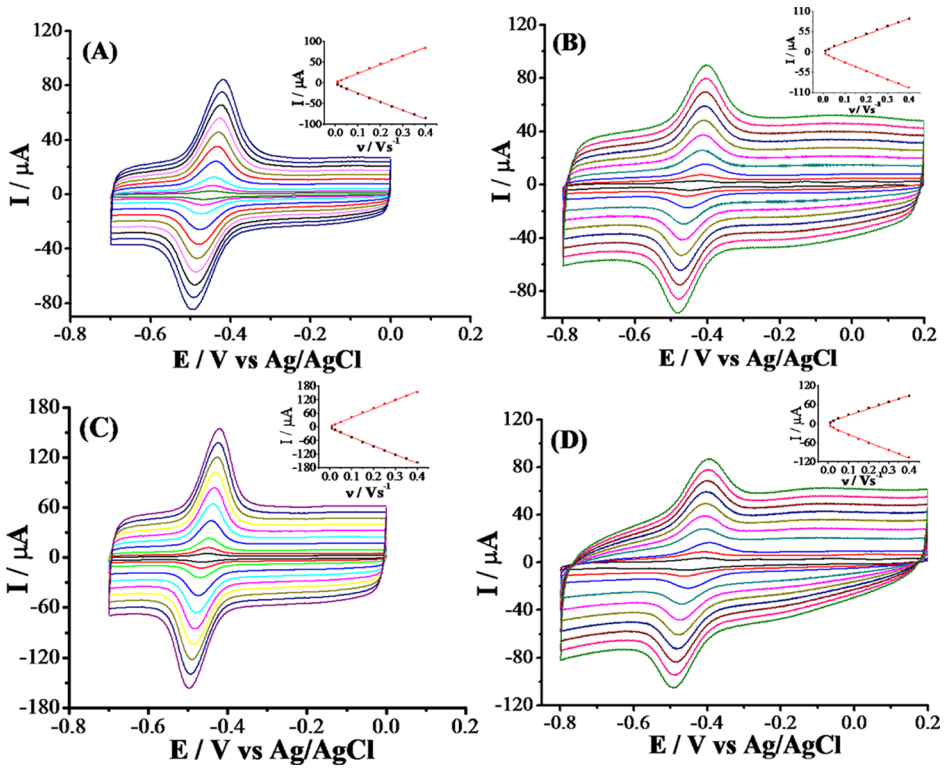

Figure 3. CVs recorded at (A) GO_X/CNT-1, (B) GO_X/CNT-2, (C) GO_X/CNT-3, and (D) GO_X/CNT-4-modified GC electrodes in an N_2-saturated 0.1 M PBS solution at different scan rates from inner to outer curves: 10, 25, 50, 100, 150, 200, 250, 300, 350, and 400 mV s^{-1}. Inset shows the linear dependence of I_{pa} and I_{pc} on the scan rate.

for GO_X/GMWNT and GO_X/DMWNT is 14 mV (ΔE_p was 47 mV for GO_X/GMWNT and 33 mV for GO_X/DMWNT).[44] This is close to the difference of ~10 mV of the ΔE_p values between GO_X/CNT-2 and GO_X/CNT-1 and between GO_X/CNT-2 and GO_X/CNT-4. The experiments were repeated several times, and the peak potentials were generally reproducible with an SD of ~7%. The electrochemical parameters for the DET of GO_X at different CNT-modified GC electrodes are given in Table 2.

The reversibility of DET of GO_X on CNT-modified GC electrodes was investigated by CVs at different scan rates under N_2-saturated conditions (Figure 3). With the increase of the scan rates, the anodic peak potentials are shifted to a more positive potential, whereas the cathodic peaks are shifted towards more

DOI: 10.1021/acsomega.7b01633
ACS Omega 2018, 3, 667−676

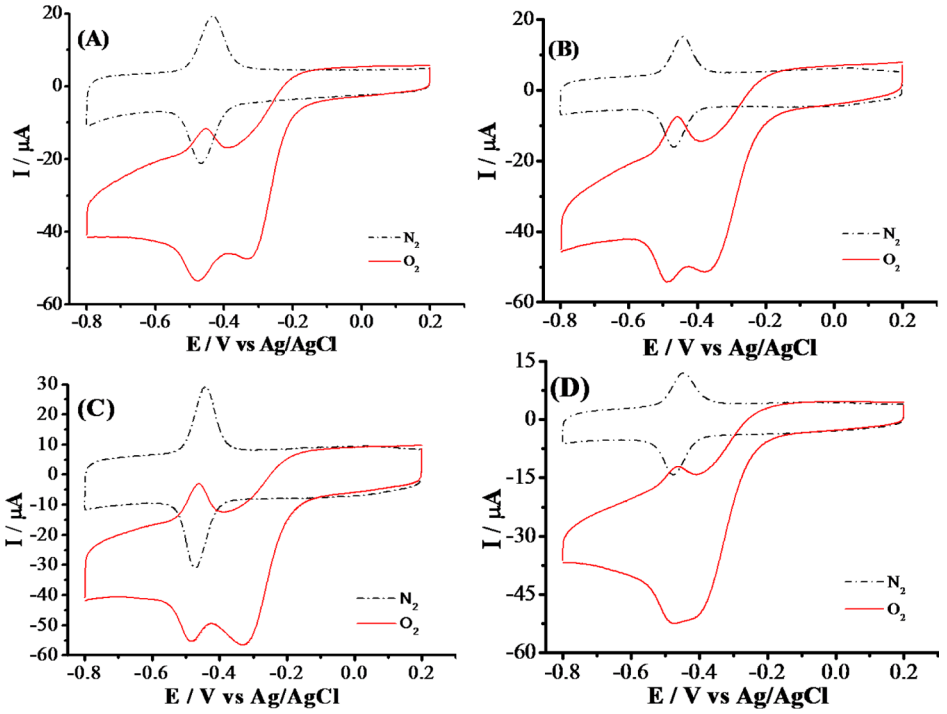

Figure 4. CVs recorded at (A) GO_X/CNT-1-, (B) GO_X/CNT-2-, (C) GO_X/CNT-3-, and (D) GO_X/CNT-4-modified GC electrodes in an N_2- and O_2-saturated 0.1 M PBS solution at a scan rate of 50 mV s^{-1}.

negative potential with no change in the formal potential, $E°$. The linear increase in the peak current with scan rates (the insets of Figure 3) demonstrates that the redox reaction of FAD/$FADH_2$ involved in the GO_X adsorbed on the CNT supports is a surface-controlled process but not a diffusion-controlled process.[7,43] The ET rate constant (k_s) can be calculated from ΔE_p using the Laviron equation for a surface-controlled electrochemical system[45] with a charge transfer coefficient (α) of 0.5. The k_s values of GO_X/CNT-modified GC electrodes were determined to be 0.984 s^{-1} for GO_X/CNT-1, 1.22 s^{-1} for GO_X/CNT-2, 1.064 s^{-1} for GO_X/CNT-3, and 1.004 s^{-1} for GO_X/CNT-4. The k_s value obtained on the GO_X/CNT-2-modified electrode is also higher than 1.16 cm s^{-1} reported by Deng et al. for the redox reaction of GO_X on the undoped CNTs but lower than 1.56 s^{-1} on boron-doped CNTs.[7] The high k_s values mean faster electron-transfer rate between the electrode and the redox-active center of the enzyme.[7] The significant dependence of the k_s on CNT supports indicates that the DET of GO_X depends on the number of walls of CNT supports, similar to that observed for alcohol oxidation and OERs in alkaline solutions.[31,32]

2.2. Electrocatalytic Activity of GO_X/CNT-Modified GC Electrodes. Figure 4 shows the electrochemical behavior of the GO_X/CNT-modified GC electrodes in N_2- and O_2-saturated PBS solutions. There are two clearly separated reduction peaks for the reaction on the GO_X/CNT-modified GC electrodes in O_2-saturated PBS solutions, except that on GO_X/CNT-4. The first one around −0.35 V is most likely associated with the reduction reaction of O_2 by CNTs. This is consistent with an early study that except MWNTs, pristine CNTs have a considerable electrochemical activity for the O_2 reduction reaction (ORR).[46] This appears to be supported by the observation of a broad reduction peak at −0.4 V for the reaction on GO_X/CNT-4-modified GC electrodes, which is consistent with the observed oxygen reduction shoulder near −0.4 V on gelatin- and DMF-dispersed MWNT-modified GC electrodes.[44] The second one around −0.45 V is the O_2 reduction peak by GO_X. However, the reduction peak current of the GO_X/CNT-modified GC electrodes increases significantly in O_2-saturated PBS solution, as compared with that recorded under N_2-saturated conditions, with subsequently reduced oxidation current. This implies that GO_X immobilized on CNTs catalyzes O_2 reduction effectively because of the fact that O_2 is a cosubstrate of GO_X. The direct electrochemistry of GO_X is a two-electron two-proton process and undergoes a redox reaction between GO_X(FAD) and $GO_X(FADH_2)$. $FADH_2$ could be oxidized by O_2 at the GO_X/CNT-modified GC electrodes, which causes the increase of the reduction peak current of GO_X (FAD)

$$\begin{array}{l} GO_X(FAD) + 2e + 2H^+ \leftrightarrow GO_X(FADH_2) \\ \uparrow \qquad\qquad\qquad\qquad \downarrow \\ GO_X(FADH_2) + O_2 \rightarrow GO_X(FAD) + H_2O_2 \end{array} \quad (1)$$

This is consistent with other studies on different GO_X-immobilized electrodes.[6,7]

The reduction peak currents at the GO_X/CNT-modified GC electrodes decrease gradually with the addition of glucose in an O_2-saturated PBS solution (Figure 5). This indicates that GO_X immobilized on CNTs retains its bioelectrocatalytic activity to glucose because of the fact that glucose is the natural substrate of GO_X.[6] The presence of glucose will lead to an enzyme-catalyzed reaction and decrease the concentration of the oxidized form of GO_X, that is, GO_X(FAD), and thus the decrease of the reduction current.

$$GO_X(FAD) + \text{glucose} \rightarrow GO_X(FADH_2) + \text{gluconolactone} \quad (2)$$

To further investigate the effect of different CNT supports on the current response of the GO_X/CNT-based glucose biosensor,

DOI: 10.1021/acsomega.7b01633
ACS Omega 2018, 3, 667−676

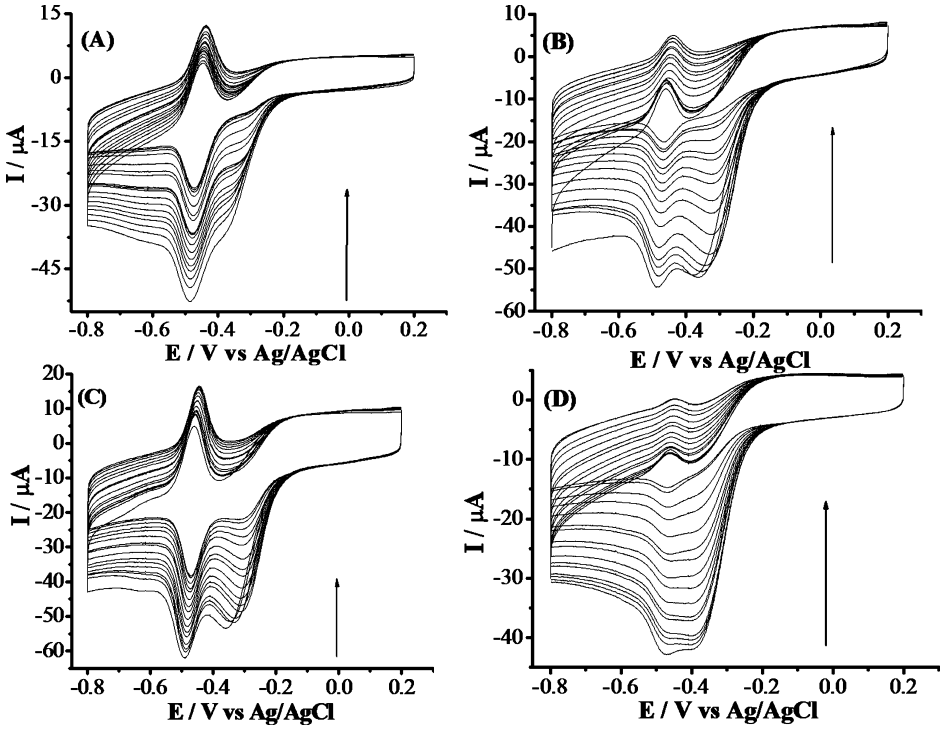

Figure 5. CVs of (A) GO_X/CNT-1, (B) GO_X/CNT-2, (C) GO_X/CNT-3, and (D) GO_X/CNT-4-modified GC electrodes in an O_2-saturated 0.1 M PBS solution at different concentrations of glucose (with 0, 100, 200, 300, 400, 600, 800, 1000, 1200, 1400, 1600, 1800, 2000, 2200, 2400, and 2600 μL of 0.1 M glucose solution into 40 mL of PBS solution from outer to inner curves).

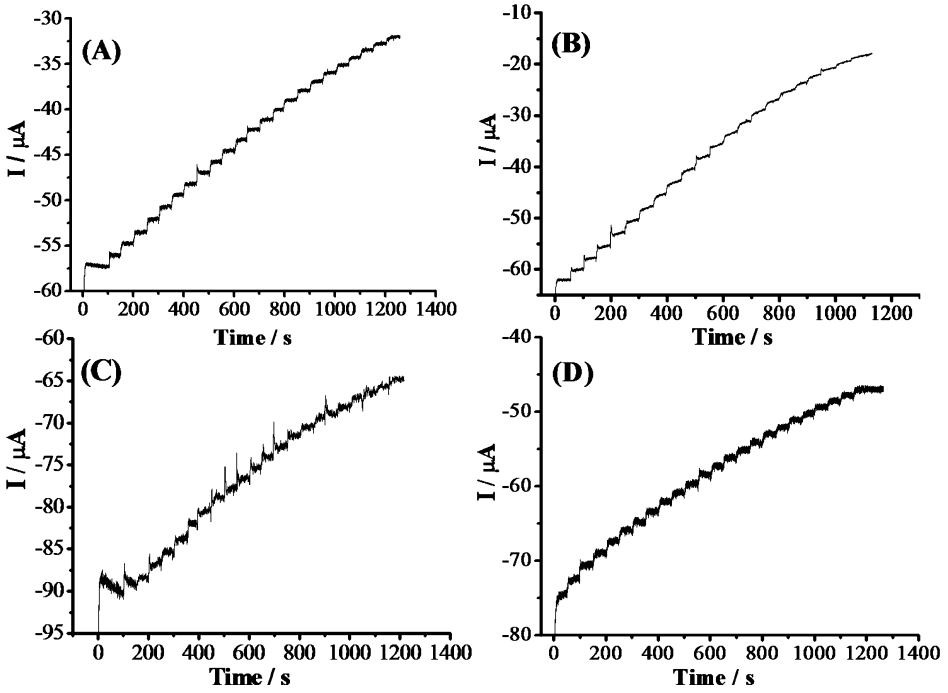

Figure 6. Amperometric responses of (A) GO_X/CNT-1-, (B) GO_X/CNT-2-, (C) GO_X/CNT-3-, and (D) GO_X/CNT-4-modified GC electrodes to successive additions of 100 μL of 0.1 M glucose to 40 mL of 0.1 M PBS solution. Solution was stirred at 150 rpm. Applied potential: −0.48 V vs Ag/AgCl.

the amperometric responses of GO_X/CNT-modified GC electrodes have been determined on successive injections of glucose to an O_2-saturated 0.1 M PBS solution under an applied potential of −0.48 V versus Ag/AgCl. As shown in Figure 6, the reduction currents decrease with the increase of the glucose concentration. On the basis of the decrease of the reduction current, the concentration of glucose can be detected. Therefore, the GO_X/CNT-modified GC electrode can be used as a glucose biosensor. Figure 7 shows the corresponding plots of the reduction current measured at −0.48 V at GO_X/CNT-modified GC electrodes versus the glucose concentration. The reduction currents of GO_X/CNT-modified GC electrodes change linearly with the concentration of glucose up to 4.31−5.44 mM, with a correlation coefficient greater than 0.994. The sensitivity of the

DOI: 10.1021/acsomega.7b01633
ACS Omega 2018, 3, 667−676

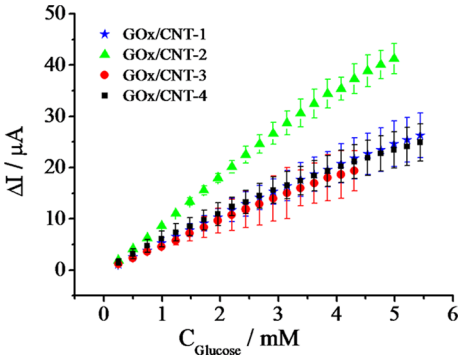

Figure 7. Current changes obtained from the amperometric curves of about the four electrodes in the different glucose concentrations in 0.1 M PBS solution. Solution was stirred at 150 rpm. Applied potential: −0.48 V vs Ag/AgCl.

GO_X/CNT-modified GC electrodes is calculated to be 37.38 ± 5.75, 66.11 ± 5.06, 35.75 ± 2.23, and 36.77 ± 4.88 μA mM^{-1} cm^{-2} on GO_X-immobilized CNT-1-, CNT-2-, CNT-3-, and CNT-4-modified GC electrodes, respectively. The sensitivity obtained on GO_X/CNT-4 is close to 40.14 μA mM^{-1} cm^{-2}, which is reported on GO_X immobilized on undoped MWNTs.[7] Similar to k_s, the highest sensitivity is obtained on GO_X immobilized on TWNTs, GO_X/CNT-2.

The apparent Michaelis−Menten constant (K_M^{app}) is an indicator of the enzymatic activity of the immobilized GO_X and can be estimated by the Lineweaver−Burk equation[8]

$$\frac{1}{i_{SS}} = \frac{1}{i_{max}} + \frac{K_M^{app}}{i_{max}} \times \frac{1}{C_{glucose}} \quad (3)$$

where i_{SS} is the steady-state response current after the addition of the substrate, i_{max} is the maximum current under saturated substrate conditions, and $C_{glucose}$ is the bulk glucose concentration. Under the conditions of this study, and K_M^{app} of GO_X/CNT-modified GC electrodes is estimated to be in the range of 6.53−11.49 mM. The low K_M^{app} value implies a strong ability of substrate binding and high enzymatic activity of the immobilized GO_X. Consistent with the high transfer rate and high sensitivity, the GO_X/CNT-2-modified GC electrode exhibits the smallest K_M^{app} value, 6.53 ± 0.58 mM, indicating that the GO_X immobilized on the TWNTs maintains an excellent catalyst activity and exhibits fabulous affinity toward glucose. Table 3 summarizes the sensitivity and K_M^{app} values of GO_X/CNT-modified GC electrodes.

2.3. Role of the Number of Walls of CNT Supports.

Before the discussion of the role of the number of inner tubes on the electrochemical behavior of GO_X immobilized on CNTs, it is necessary to clarify the effect of the surface areas and residual metal impurities of CNTs used in this study. In catalysis, the electrocatalytic activity of catalysts is generally normalized with the surface area of the catalytic NPs to eliminate or avoid the effect of the size of the catalysts. It is well-known that the size of supported catalytic NPs plays a determining role in their activity and stability, and the catalytic specific activity usually increases with the decreasing NP size because of the rising number of low-coordinated metal atoms and/or defects as the catalytically active sites.[47,48] In this study, the BET surface area of CNTs is close for CNTs with the number of layers from 1 to 7: 577, 523, and 539 m^2 g^{-1} for CNT-1, CNT-2, and CNT-3 (see Table 1), respectively. Only in the case of CNTs with 12 layers (CNT-4, MWNTs), the surface area decreased significantly to 271 m^2 g^{-1}. This indicates that if the surface area of CNT substrates is a dominant fact in the electrochemical behavior of GO_X/CNTs, the electrochemical activity of GO_X/CNTs should be similar at least for GO_X immobilized on CNT-1, CNT-2, and CNT-3. However, this is not the case, as shown in this study, and the electrocatalytic activity of GO_X/CNTs depends strongly on CNT-1, CNT-2, and CNT-3, and the best results were obtained on GO_X/CNT-2, even though the surface area of CNT-2 is actually slightly lower than that of CNT-1. Despite the fact that the surface area of CNT-1 is much higher than that of CNT-4, their k_s, sensitivities, and K_M^{app} values are very close (Tables 2 and 3). Therefore, the surface area is not a dominant factor in the DET and electrocatalytic activity of GO_X/CNT-modified GC electrodes. The amounts of metallic impurities of CNT supports after purification are less than 100 ppm.[32] As shown in Figure 2A, pristine CNTs show no redox peaks in 0.1 M PBS solution, indicating that such low levels of metallic impurities in CNTs do not contribute to the electrochemical properties of GO_X.

As shown by Marcus and Sutin, the ET rate exponentially depends on the distance of the closest approach between an electron donor and acceptor and is negligible for distances beyond 2 nm.[49] This indicates that the DET of FAD active sites deeply embedded (~1.5 nm) within the protein to the electrode surfaces would be very difficult. This is supported by the featurelessness of the CV curves of GO_X-modified GC electrodes without immobilization of CNTs (Figure 2B). It has been well-known that CNTs promote the DET to GO_X.[3,7,18−20,22,50] However, the results of the current study demonstrate for the first time that the direct electrochemistry and DET of redox centers of GO_X immobilized on CNTs also depend critically on the nature of CNT supports, that is, the number of walls or inner tubes. Among the CNTs studied, CNT-2 shows the best results to enhance the DET and the biocatalytic activity of GO_X toward glucose, showing the highest k_s, highest sensitivity, and lowest K_M^{app} value.

As shown early, pristine CNTs are inherently electrocatalytically active for the OER, ORR, and H_2 evolution reaction (HER) in alkaline solutions, showing a distinct volcano-type curve as a function of the number of inner tubes or walls.[31,46] The intrinsic activity of pristine CNTs has been evidently demonstrated by the KCN blockage experiments, in which cyanide ions, CN^{-1}, strongly coordinate with transition metals such as Co, Fe, and Ni in the axial position,[51,52] thus completely blocking and poisoning

Table 3. Parameters Estimated from the Amperometric Response for the Different GO_X/CNT-Modified GC Electrodes in Glucose Solutions

electrode	K_M^{app} (mM)	sensitivity (μA mM^{-1} cm^{-2})	linear range (mM)	linear regression equations
GO_X/CNT-1	9.24 ± 1.5	37.38 ± 5.73	0.25−5.44	$y = 4.8828x + 0.6025$ ($R^2 = 0.9971$)
GO_X/CNT-2	6.53 ± 0.58	66.11 ± 5.06	0.25−4.99	$y = 8.5424x + 0.7412$ ($R^2 = 0.9948$)
GO_X/CNT-3	9.01 ± 1.45	35.75 ± 2.23	0.25−4.31	$y = 4.5977x + 0.2929$ ($R^2 = 0.9973$)
GO_X/CNT-4	11.49 ± 3.01	36.77 ± 4.88	0.25−4.99	$y = 4.5751 + 1.6219$ ($R^2 = 0.9936$)

DOI: 10.1021/acsomega.7b01633
ACS Omega 2018, 3, 667−676

the metallic impurities on the side walls of CNTs. In the presence of KCN, CNTs show distinctive activity volcano curves, which are identical to those observed on the pristine CNTs in the absence of KCN.[46] This evidently demonstrates that the inner tubes of CNTs play a significant role in the enhancement of the charge transfer of the reactions such as OER, ORR, and HER via the electron-tunneling effect between the outer and inner walls.[46]

The strong promotion effect of inner tubes on the electrocatalytic activity of CNTs has also demonstrated the electrooxidation of alcohols on Pt and Pd NPs supported on CNTs, with highest activities observed on Pt and Pd NPs supported on CNTs with 2−3 walls.[32−34] As shown in Figure 8, the k_s and

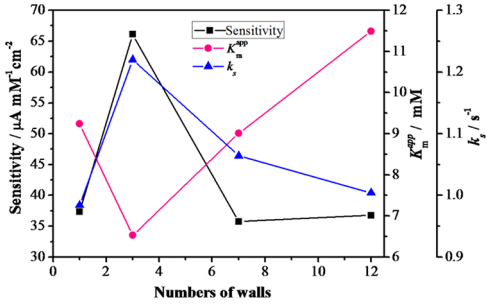

Figure 8. Plots of electrocatalytic activity of GO_X/CNT-modified GC electrodes as a function of the number of inner tubes of CNT substrates.

sensitivity values show distinctive volcano curves, whereas the K_M^{app} values exhibit a reversed volcano curve as a function of the number of walls, identical to that observed for alcohol oxidation and OERs in alkaline solutions.[31−33] A high k_s value of 1.22 s^{-1} obtained for the DET of GO_X/CNT-2 indicates the fast ET for the direct electrochemistry of GO_X immobilized on TWNTs, as compared to that immobilized on conventional SWNTs and MWNTs. The observation of the distinguished volcano-type curves of the electrocatalytic activity of GO_X/CNTs in this study and that of pristine CNTs and Pt and Pd NPs supported on CNTs as a function of number of inner tubes or walls, despite the significant differences in the electrochemical systems, clearly indicates the existence of the inherent electrocatalytic activities of CNTs. The promotion effect of inner tubes has also been demonstrated most recently on the dye-functionalized CNTs for PEC water splitting, in which the dye-functionalized DWNTs and TWNTs show a much higher PEC activity for water splitting as compared to that of SWNTs and MWNTs.[35] In other words, the promotion effect of CNTs via the electron-tunneling mechanism is an intrinsic property of CNTs with a defined number of walls. Thus, the reason for the observation of the highest DET and electrocatalytic activity of GO_X immobilized on CNT-2, a mixture of TWNTs and DWNTs, is most likely the facile charge-transfer process via the electron tunneling between the outer wall and inner tubes of CNT-2 under the influence of an electrochemical driving force, which is consistent with previous studies.[31−34,46] Figure 9 shows schematically the DET of the redox-active center of GO_X and CNTs facilitated by the electron tunneling between the outer wall and inner tubes of CNTs.

Similar to the electrochemical reactions of OER on CNTs,[31,46] such effective charge or ET as described above would not be possible for the GO_X supported on SWNTs and GO_X/CNT-1 and diminishes as the number of walls increases because of the significantly reduced polarization driving force or dc bias across the walls or layers of CNTs for the ET between the outer wall and

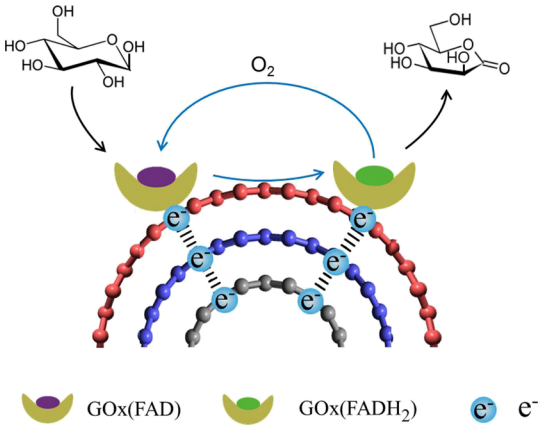

Figure 9. Scheme of the DET and electrocatalytic activity of GO_X immobilized on TWNTs via the electron-tunneling mechanism between the outer wall and inner tubes of TWNTs.

inner tubes. Thus, the ET efficiency of the redox reaction of GO_X immobilized on CNT-2, a mixture of DWNTs and TWNTs, is much higher when the ET is between the outer wall and inner tubes as compared to that on SWNTs and MWNTs, GO_X/CNT-1, and GO_X/CNT-4.

As pointed out by Chen et al., the structural factors such as the number of layers, size, and chirality, and layer stacking modes can significantly alter the heterogeneous electron-transfer efficiency at sp^2 nanocarbons such as graphene and CNTs.[53,54] CNTs act as electrical conducting nanowires for the fast DET between the active sites in GO_X and substrate electrodes. The electron tunneling or transfer efficiency between CNTs and the GO_X active sites depends on the density of states (DOS) and the layers of CNTs. For SWNTs, the DOS is rather low near their Fermi levels, and therefore, the ET efficiency is very low. Increasing the wall numbers would increase the DOS near the Fermi level, which would increase the ET efficiency. On the other hand, however, the increase of wall numbers (thickness) of CNTs could increase the ET distance, which could lower the ET efficiency. Thus, CNTs with 2−3 walls may provide an optimized balance between these two effects. This also explains the observed high electrocatalytic activity of CNT-2 toward glucose.

3. CONCLUSIONS

In the present study, we studied in detail the effect of CNT supports on the DET and electrocataytic activities of GO_X in 0.1 M PBS solution. A pair of well-defined and fundamentally reversible redox peaks was observed, indicating an excellent DET between the redox centers of GO_X and GC electrodes without the help of the electron-transfer mediators or metallic NPs to contact the FAD active centers. Furthermore, the GO_X immobilized by the CNTs still maintained its biocatalytic activity toward glucose. However, the direct electrochemistry and electrocatalytic activity of GO_X depend strongly on the nature of CNT supports, showing distinct volcano curves as a function of the number of walls. GO_X immobilized on CNT-2, a mixture of TWNTs and DWNTs, is most effective in promoting the DET and electrocatalytic activity toward glucose, showing the highest k_s value and sensitivity and the lowest K_M^{app}. The excellent promotion effect of CNT-2 is ascribed to the fast DET via the efficient electron tunneling between the outer wall and inner tubes of CNTs. The results demonstrate that the DET and electrocatalytic activities of GO_X immobilized on CNTs can be manipulated by the quantum properties of CNT supports. This

DOI: 10.1021/acsomega.7b01633
ACS Omega 2018, 3, 667−676

has general implications for the fundamental understanding of the role of CNT supports in the DET or ET processes, and the results can be used for the better design of biocatalysts for biofuel cell and biosensor applications. For the development of practical biocatalysts, the addition of electrocatalysts would be beneficial to further increase the activity and sensitivity. However, as shown in the present study, the use of CNT supports with 2−3 inner tubes would significantly enhance the activity and sensitivity of the electrocatalysts in applications such as biofuel cells and glucose biosensors.

4. EXPERIMENTAL SECTION

4.1. Materials and Solutions. Glucose oxidase (GO_X, EC 1.1.3.4, 100−250 U/mg, type X-S from *Aspergillus niger*), D-(+)-glucose, DMF, sodium phosphate monobasic, and sodium phosphate dibasic were purchased from Sigma Aldrich. Nafion solution (5 wt % in isopropanol and water) was purchased from DuPont Inc. Four CNTs with different number of walls were purchased from Nanostructured & Amorphous Materials Inc., USA. Deionized double-distilled water (18.6 MΩ, Millipore) was used throughout the experiment.

CNTs were purified using ultrasonic treatment in 32 wt % HCl solution (Ajax Finechem) for 6 h and then stirred at room temperature for 48 h. CNTs were characterized by TEM (JEOL 3000F) with an operation voltage of 200 kV, and the BET surface area of CNTs was measured by Micromeritics TriStar II. PBS solutions (0.1 M, pH 7.4) were prepared by mixing 0.1 M NaH_2PO_4 and 0.1 M Na_2HPO_4, and the pH of the solution was adjusted by adding H_3PO_4 or NaOH. Glucose stock solution was prepared by PBS solution and stored for at least 24 h at room temperature before use. CNTs (∼2 mg) were dispersed into 5 mL DMF and then ultrasonicated for 1 h to form a stable CNT suspension. GO_X solution (10 mg mL^{-1}) was stored in −4 °C. All aqueous solutions were prepared with double-distilled deionized water.

4.2. Preparation of GO_X/CNT-Modified Electrodes. The 4.0 mm diameter GC electrode was polished with 3 μm alumina powder and sonicated in deionized water for 5 min, and it served as the working electrode. After drying, the GO_X/CNT film electrodes were prepared by successively casting 5 μL of CNT suspensions and GO_X solution on the electrode surface. After CNTs and GO_X solution deposition, the solvent was allowed to evaporate at room temperature. To protect the working electrode, 5 μL of Nafion solution was dropped on the surface of the cast electrode films and dried at room temperature.

4.3. Characterization. Electrochemical measurements were performed in a conventional three-electrode cell with an Ag/AgCl reference electrode and a Pt counter electrode in N_2- or O_2-saturated 0.1 M PBS solution, using a CHI6044D electrochemical work station. The Ag/AgCl reference electrode was kept in saturated KCl solution. CVs of the bare GC and GO_X/CNT-modified GC electrodes were generally obtained at a scan rate of 50 mV s^{-1}. The amperometric measurements were performed at a fixed potential (−0.48 V vs Ag/AgCl). Glucose (100 μL, 0.1 M) was directly added to 40 mL of 0.1 M PBS solution at 0 s with the successive increase of the glucose concentration (100 μL, 0.1 M glucose). The reason for performing the amperometric measurements at this fixed potential is to maximize the activity and sensitivity of measurements, as −0.48 V is close to the cathodic peak potential of direct electrochemistry of GO_X/CNT-modified GC, as shown in the results section. The experiments were repeated at least three times, and the results were presented as the average values.

AUTHOR INFORMATION

Corresponding Author

*E-mail: s.jiang@curtin.edu.au (S.P.J.).

ORCID

San Ping Jiang: 0000-0002-7042-2976

Notes

The authors declare no competing financial interest.

ACKNOWLEDGMENTS

This work was financially supported by the Australian Research Council under Discovery Project scheme (Project numbers: DP150102044, DP150102025, DP180100568, and DP180100731). The authors acknowledge the facilities and the scientific and technical assistance of the National Imaging Facility at the Centre for Microscopy, Characterisation & Analysis, the University of Western Australia, a facility funded by the University and State and Commonwealth Government.

REFERENCES

(1) Das, D.; Ghosh, S.; Basumallick, I. Electrochemical Studies on Glucose Oxidation in an Enzymatic Fuel Cell with Enzyme Immobilized on to Reduced Graphene Oxide Surface. *Electroanalysis* **2014**, *26*, 2408−2418.

(2) Krikstolaityte, V.; Oztekin, Y.; Kuliesius, J.; Ramanaviciene, A.; Yazicigil, Z.; Ersoz, M.; Okumus, A.; Kausaite-Minkstimiene, A.; Kilic, Z.; Solak, A. O.; Makaraviciute, A.; Ramanavicius, A. Biofuel Cell Based on Anode and Cathode Modified by Glucose Oxidase. *Electroanalysis* **2013**, *25*, 2677−2683.

(3) Leech, D.; Kavanagh, P.; Schuhmann, W. Enzymatic Fuel Cells: Recent Progress. *Electrochim. Acta* **2012**, *84*, 223−234.

(4) Sarma, A. K.; Vatsyayan, P.; Goswami, P.; Minteer, S. D. Recent Advances in Material Science for Developing Enzyme Electrodes. *Biosens. Bioelectron.* **2009**, *24*, 2313−2322.

(5) Liu, Y.; Du, Y.; Li, C. M. Direct Electrochemistry Based Biosensors and Biofuel Cells Enabled with Nanostructured Materials. *Electroanalysis* **2013**, *25*, 815−831.

(6) Xu, Q.; Gu, S.-X.; Jin, L.; Zhou, Y.-e.; Yang, Z.; Wang, W.; Hu, X. Graphene/Polyaniline/Gold Nanoparticles Nanocomposite for the Direct Electron Transfer of Glucose Oxidase and Glucose Biosensing. *Sens. Actuators, B* **2014**, *190*, 562−569.

(7) Deng, C.; Chen, J.; Chen, X.; Xiao, C.; Nie, L.; Yao, S. Direct Electrochemistry of Glucose Oxidase and Biosensing for Glucose Based on Boron-Doped Carbon Nanotubes Modified Electrode. *Biosens. Bioelectron.* **2008**, *23*, 1272−1277.

(8) du Toit, H.; Di Lorenzo, M. Glucose Oxidase Directly Immobilized onto Highly Porous Gold Electrodes for Sensing and Fuel Cell Applications. *Electrochim. Acta* **2014**, *138*, 86−92.

(9) Wang, K.; Liu, Y.; Chen, S. Improved Microbial Electrocatalysis with Neutral Red Immobilized Electrode. *J. Power Sources* **2011**, *196*, 164−168.

(10) de Poulpiquet, A.; Ciaccafava, A.; Lojou, E. New Trends in Enzyme Immobilization at Nanostructured Interfaces for Efficient Electrocatalysis in Biofuel Cells. *Electrochim. Acta* **2014**, *126*, 104−114.

(11) Krajewska, B. Application of Chitin- and Chitosan-Based Materials for Enzyme Immobilizations: A Review. *Enzyme Microb. Technol.* **2004**, *35*, 126−139.

(12) Harper, A.; Anderson, M. R. Electrochemical Glucose Sensors—Developments Using Electrostatic Assembly and Carbon Nanotubes for Biosensor Construction. *Sensors* **2010**, *10*, 8248−8274.

(13) Chen, J.; Zheng, X.; Miao, F.; Zhang, J.; Cui, X.; Zheng, W. Engineering Graphene/Carbon Nanotube Hybrid for Direct Electron Transfer of Glucose Oxidase and Glucose Biosensor. *J. Appl. Electrochem.* **2012**, *42*, 875−881.

(14) Ho, P. I.; Kumar, G. G.; Kim, A. R.; Kim, P.; Nahm, K. S. Microbial Electricity Generation of Diversified Carbonaceous Electrodes under Variable Mediators. *Bioelectrochemistry* **2011**, *80*, 99−104.

DOI: 10.1021/acsomega.7b01633
ACS Omega 2018, 3, 667−676

(15) Tanaka, K.; Tamamushi, R. Effect of Hydrophobic Layers on the Electrochemical Electron-Transfer Reaction of Some Mediators in Microbial Fuel-Cells. *J. Electroanal. Chem.* **1987**, *236*, 305−307.
(16) Walker, A. L.; Walker, C. W. Biological Fuel Cell and an Application as a Reserve Power Source. *J. Power Sources* **2006**, *160*, 123−129.
(17) Fishilevich, S.; Amir, L.; Fridman, Y.; Aharoni, A.; Alfonta, L. Surface Display of Redox Enzymes in Microbial Fuel Cells. *J. Am. Chem. Soc.* **2009**, *131*, 12052−12053.
(18) Gao, F.; Viry, L.; Maugey, M.; Poulin, P.; Mano, N. Engineering Hybrid Nanotube Wires for High-Power Biofuel Cells. *Nat. Commun.* **2010**, *1*, 2.
(19) Ciaccafava, A.; De Poulpiquet, A.; Techer, V.; Giudici-Orticoni, M. T.; Tingry, S.; Innocent, C.; Lojou, E. An Innovative Powerful and Mediatorless H_2/O_2 Biofuel Cell Based on an Outstanding Bioanode. *Electrochem. Commun.* **2012**, *23*, 25−28.
(20) Osadebe, I.; Leech, D. Effect of Multi-Walled Carbon Nanotubes on Glucose Oxidation by Glucose Oxidase or a Flavin-Dependent Glucose Dehydrogenase in Redox-Polymer-Mediated Enzymatic Fuel Cell Anodes. *ChemElectroChem* **2014**, *1*, 1988−1993.
(21) Ma, X.; Hu, W.; Guo, C.; Yu, L.; Gao, L.; Xie, J.; Li, C. M. DNA-Templated Biomimetic Enzyme Sheets on Carbon Nanotubes to Sensitively in Situ Detect Superoxide Anions Released from Cells. *Adv. Funct. Mater.* **2014**, *24*, 5897−5903.
(22) Filip, J.; Šefčovičová, J.; Gemeiner, P.; Tkac, J. Electrochemistry of Bilirubin Oxidase and Its Use in Preparation of a Low Cost Enzymatic Biofuel Cell Based on a Renewable Composite Binder Chitosan. *Electrochim. Acta* **2013**, *87*, 366−374.
(23) Haneda, K.; Yoshino, S.; Ofuji, T.; Miyake, T.; Nishizawa, M. Sheet-Shaped Biofuel Cell Constructed from Enzyme-Modified Nano-engineered Carbon Fabric. *Electrochim. Acta* **2012**, *82*, 175−178.
(24) Lesniewski, A.; Paszewski, M.; Opallo, M. Gold-Carbon Three Dimensional Film Electrode Prepared from Oppositely Charged Conductive Nanoparticles by Layer-by-Layer Approach. *Electrochem. Commun.* **2010**, *12*, 435−437.
(25) Hu, F. X.; Kang, Y. J.; Du, F.; Zhu, L.; Xue, Y. H.; Chen, T.; Dai, L. M.; Li, C. M. Living Cells Directly Growing on a DNA/Mn3(Po4)2-Immobilized and Vertically Aligned Cnt Array as a Free-Standing Hybrid Film for Highly Sensitive in Situ Detection of Released Superoxide Anions. *Adv. Funct. Mater.* **2015**, *25*, 5924−5932.
(26) Shi, Z.; Wu, X.; Gao, L.; Tian, Y.; Yu, L. Electrodes/Paper Sandwich Devices for in Situ Sensing of Hydrogen Peroxide Secretion from Cells Growing in Gels-in-Paper 3-Dimensional Matrix. *Anal. Methods* **2014**, *6*, 4446−4454.
(27) Yang, X.-Y.; Tian, G.; Jiang, N.; Su, B.-L. Immobilization Technology: A Sustainable Solution for Biofuel Cell Design. *Energy Environ. Sci.* **2012**, *5*, 5540−5563.
(28) Dong, C.; Campell, A. S.; Eldawud, R.; Perhinschi, G.; Rojanasakul, Y.; Dinu, C. Z. Effects of Acid Treatment on Structure, Properties and Biocompatibility of Carbon Nanotubes. *Appl. Surf. Sci.* **2013**, *264*, 261−268.
(29) Feng, W.; Ji, P. Enzymes Immobilized on Carbon Nanotubes. *Biotechnol. Adv.* **2011**, *29*, 889−895.
(30) Pang, R.; Li, M.; Zhang, C. Degradation of Phenolic Compounds by Laccase Immobilized on Carbon Nanomaterials: Diffusional Limitation Investigation. *Talanta* **2015**, *131*, 38−45.
(31) Cheng, Y.; Xu, C.; Jia, L.; Gale, J. D.; Zhang, L.; Liu, C.; Shen, P. K.; Jiang, S. P. Pristine Carbon Nanotubes as Non-Metal Electrocatalysts for Oxygen Evolution Reaction of Water Splitting. *Appl. Catal., B* **2015**, *163*, 96−104.
(32) Zhang, J.; Cheng, Y.; Lu, S.; Jia, L.; Shen, P. K.; Jiang, S. P. Significant Promotion Effect of Carbon Nanotubes on the Electrocatalytic Activity of Supported Pd Nps for Ethanol Oxidation Reaction of Fuel Cells: The Role of Inner Tubes. *Chem. Commun.* **2014**, *50*, 13732−13734.
(33) Yuan, W.; Cheng, Y.; Shen, P. K.; Li, C. M.; Jiang, S. P. Significance of Wall Number on the Carbon Nanotube Support-Promoted Electrocatalytic Activity of Pt Nps Towards Methanol/Formic Acid Oxidation Reactions in Direct Alcohol Fuel Cells. *J. Mater. Chem. A* **2015**, *3*, 1961−1971.
(34) Zhang, J.; Lu, S.; Xiang, Y.; Shen, P. K.; Liu, J.; Jiang, S. P. Carbon-Nanotubes-Supported Pd Nanoparticles for Alcohol Oxidations in Fuel Cells: Effect of Number of Nanotube Walls on Activity. *Chemsuschem* **2015**, *8*, 2956−2966.
(35) Cheng, Y.; Memar, A.; Saunders, M.; Pan, J.; Liu, C.; Gale, J. D.; Demichelis, R.; Shen, P. K.; Jiang, S. P. Dye Functionalized Carbon Nanotubes for Photoelectrochemical Water Splitting—Role of Inner Tubes. *J. Mater. Chem. A* **2016**, *4*, 2473−2483.
(36) Kim, T.; Kim, G.; Choi, W. I.; Kwon, Y.-K.; Zuo, J.-M. Electrical Transport in Small Bundles of Single-Walled Carbon Nanotubes: Intertube Interaction and Effects of Tube Deformation. *Appl. Phys. Lett.* **2010**, *96*, 173107.
(37) Wen, D.; Liu, Y.; Yang, G.; Dong, S. Electrochemistry of Glucose Oxidase Immobilized on the Carbon Nanotube Wrapped by Polyelectrolyte. *Electrochim. Acta* **2007**, *52*, 5312−5317.
(38) Yang, D.-Q.; Rochette, J.-F.; Sacher, E. Spectroscopic Evidence for π-π Interaction between Poly(Diallyl Dimethylammonium) Chloride and Multiwalled Carbon Nanotubes. *J. Phys. Chem. B* **2005**, *109*, 4481−4484.
(39) Katz, E. Application of Bifunctional Reagents for Immobilization of Proteins on a Carbon Electrode Surface:Oriented Immobilization of Photosynthetic Reaction Centers. *J. Electroanal. Chem.* **1994**, *365*, 157−164.
(40) Wang, S.; Jiang, S. P.; Wang, X. Polyelectrolyte Functionalized Carbon Nanotubes as a Support for Noble Metal Electrocatalysts and Their Activity for Methanol Oxidation. *Nanotechnology* **2008**, *19*, 265601.
(41) Xiang, Y.; Lu, S.; Jiang, S. P. Layer-by-Layer Self-Assembly in the Development of Electrochemical Energy Conversion and Storage Devices from Fuel Cells to Supercapacitors. *Chem. Soc. Rev.* **2012**, *41*, 7291−7321.
(42) Periasamy, A. P.; Chang, Y.-J.; Chen, S.-M. Amperometric Glucose Sensor Based on Glucose Oxidase Immobilized on Gelatin-Multiwalled Carbon Nanotube Modified Glassy Carbon Electrode. *Bioelectrochemistry* **2011**, *80*, 114−120.
(43) Oztekin, Y.; Ramanaviciene, A.; Yazicigil, Z.; Solak, A. O.; Ramanavicius, A. Direct Electron Transfer from Glucose Oxidase Immobilized on Polyphenanthroline-Modified Glassy Carbon Electrode. *Biosens. Bioelectron.* **2011**, *26*, 2541−2546.
(44) Periasamy, A. P.; Chang, Y.-J.; Chen, S.-M. Amperometric Glucose Sensor Based on Glucose Oxidase Immobilized on Gelatin-Multiwalled Carbon Nanotube Modified Glassy Carbon Electrode. *Bioelectrochemistry* **2011**, *80*, 114−120.
(45) Laviron, E. General Expression of the Linear Potential Sweep Voltammogram in the Case of Diffusionless Electrochemical Systems. *J. Electroanal. Chem. Interfacial Electrochem.* **1979**, *101*, 19−28.
(46) Cheng, Y.; Zhang, J.; Jiang, S. P. Are Metal-Free Pristine Carbon Nanotubes Electrocatalytically Active? *Chem. Commun.* **2015**, *51*, 13764−13767.
(47) Mistry, H.; Reske, R.; Zeng, Z.; Zhao, Z.-J.; Greeley, J.; Strasser, P.; Cuenya, B. R. Exceptional Size-Dependent Activity Enhancement in the Electroreduction of Co2 over Au Nanoparticles. *J. Am. Chem. Soc.* **2014**, *136*, 16473−16476.
(48) Wang, S.; Jiang, S. P.; White, T. J.; Guo, J.; Wang, X. Electrocatalytic Activity and Interconnectivity of Pt Nanoparticles on Multiwalled Carbon Nanotubes for Fuel Cells. *J. Phys. Chem. C* **2009**, *113*, 18935−18945.
(49) Marcus, R. A.; Sutin, N. Electron Transfers in Chemistry and Biology. *Biochim. Biophys. Acta* **1985**, *811*, 265−322.
(50) Walcarius, A.; Minteer, S. D.; Wang, J.; Lin, Y.; Merkoçi, A. Nanomaterials for Bio-Functionalized Electrodes: Recent Trends. *J. Mater. Chem. B* **2013**, *1*, 4878−4908.
(51) Gupta, S.; Fierro, C.; Yeager, E. The Effects of Cyanide on the Electrochemical Properties of Transition-Metal Macrocycles for Oxygen Reduction Reaction in Alkaline-Solutions. *J. Electroanal. Chem.* **1991**, *306*, 239−250.

DOI: 10.1021/acsomega.7b01633
ACS Omega 2018, 3, 667−676

(52) Thorum, M. S.; Hankett, J. M.; Gewirth, A. A. Poisoning the Oxygen Reduction Reaction on Carbon-Supported Fe and Cu Electrocatalysts: Evidence for Metal-Centered Activity. *J. Phys. Chem. Lett.* **2011**, *2*, 295−298.
(53) Chen, S.; Liu, Y.; Chen, J. Heterogeneous Electron Transfer at Nanoscopic Electrodes: Importance of Electronic Structures and Electric Double Layers. *Chem. Soc. Rev.* **2014**, *43*, 5372−5386.
(54) Zhang, B.; Fan, L.; Zhong, H.; Liu, Y.; Chen, S. Graphene Nanoelectrodes: Fabrication and Size-Dependent Electrochemistry. *J. Am. Chem. Soc.* **2013**, *135*, 10073−10080.

DOI: 10.1021/acsomega.7b01633
ACS Omega 2018, 3, 667−676